

Axial-vector form factor of nucleons at finite temperature from the AdS/QCD soft-wall model

Shahin Mamedov^{a,b} ¹ and Narmin Nasibova^b ²

^a *Institute for Physical Problems, Baku State University,*

Z. Khalilov str. 23, Baku, AZ1148, Azerbaijan

^b *Institute of Physics, Azerbaijan National Academy of Sciences,*

AZ1143, H. Javid avenue 131, Baku, Azerbaijan

Abstract

The axial-vector form factor of the nucleons is considered at finite temperature using the holographic soft-wall model having the thermal dilaton field. We use bulk interaction action known from the zero temperature case and apply in it the profile functions of fields, which are thermalized by both AdS-Schwarzschild metric and by the interaction with the thermal dilaton. Dependencies from the squared momentum transfer and the temperature are plotted for the ground and excited states of the nucleons.

I. INTRODUCTION

In the weak processes, such as β decay $n \rightarrow p + e^- + \bar{\nu}_e$ and μ capture $\mu^- + p = \nu_\mu + n$, an interaction takes place with the axial-vector current of the baryons. The form factor $G_A(Q^2)$, which describes the interaction vertex in these processes, is called the axial-vector form factor of the nucleons. Studying of the axial-vector form factor is also used for the interpretation of neutrino experiments [1, 2]. The G_A form factor was studied in the framework of different models of field theory (QCD sum rules, chiral quark model, etc.), for the low or high values of the Q^2 momentum transfer in the works [3–9]. After the appearance of the QCD models based on AdS/CFT corre-

¹ e-mail : sh.mamedov62@gmail.com (corresponding author)

² e-mail :n.nesibli88@gmail.com

spondence [10–12], which are called holographic QCD or AdS/QCD models [13–19] many problems of strong interactions have been reconsidered in the framework of these models. The holographic QCD enabled us to investigate the axial-vector form factor by imposing no limitation on Q^2 , i.e., to consider it at both small and big values of Q^2 . As a result, both energy areas were joined within one graph, which nicely agree with the graphs of the different approaches for the various Q^2 areas. It explains the experimental data as well. Within holographic QCD the G_A form factor was considered in the hard-wall model framework in Refs. [20–23] and in the soft-wall model framework in the Refs. [22, 24]. In the nuclear medium or the medium of the nucleons, which forms as the result of the heavy ions or proton-proton collisions, this interaction vertex will depend on quantities describing medium, such as temperature, density, and isospin chemical potential as well. In Ref. [25] the axial form factor splitting in the holographic approach has been studied in the so-called isospin medium, which is the simplified model of nuclear medium. Such a "medium" takes into account only the isospin chemical potential of the medium and neglects all other quantities. Interaction with the isospin background of the medium leads to a mass splitting of nucleons, which results the splitting the G_A form factor into two, which correspond to the different isospin projections.

Recently, in Refs. [26, 27], the finite temperature theory of mesons and baryons was considered within the soft-wall model of the AdS/QCD. Given explicit formulas for the wave functions of mesons and baryons in 5D enable us to solve 4D QCD interaction issues at finite temperatures. With the application of this approach, the hadron and electromagnetic form factors of the nucleons were studied in Refs. [26–28] and the meson-nucleon coupling constants' dependencies on temperature were found in Refs. [29, 30]. This approach enables us to study the G_A form factor in the thermal medium. The same problem was considered in Ref.[31] within the QCD sum rules framework. Here we aim to consider a temperature dependence of the axial-vector form factor neglecting all other medium quantities. This study will be useful for the neutrino- and anti-neutrino-nucleus scattering experiments Refs. [32–34].

The remainder of this paper is organized as follows:

In Section II we briefly present the definition of the axial-vector form factor at finite temperature. Section III is devoted to the basic notions in the holographic soft-wall model with the thermal dilaton field. Sections IV and V are about the equation of motions, meson bulk-to boundary propagator at finite temperature, and the profile functions of fermion fields at finite temperature. In section VI, the breaking of chiral symmetry at a finite temperature is described. In Sec. VII. we give an interaction lagrangian between the bulk fields. Using the AdS/CFT correspondence, we obtain an integral expression for the form factor. In Sec. VIII. we derive the $G_A(T)$ form factor

at a non-zero temperature from the corresponding action. In Sec. IX, the free parameters are fixed, and the axial-vector form factors' normalized graphs are plotted for the different values of the parameter α . In the last section, we summarize our results.

II. AXIAL-VECTOR CURRENT OF THE NUCLEONS

In QCD the isovector axial-vector current of nucleons is defined as follows [3]:

$$j^{\mu,a}(x) = \bar{\psi}(x) \gamma^\mu \gamma^5 \frac{\tau^a}{2} \psi(x), \quad (1)$$

where ψ is the doublet of u and d quarks $\psi = \begin{pmatrix} u \\ d \end{pmatrix}$ and τ^a are the isospin Pauli matrices. The current (1) is a partially conserved:

$$\partial_\mu j^{\mu,a}(x) = i\bar{\psi}(x) \gamma^5 \left\{ \frac{\tau^a}{2}, \mu \right\} \psi(x). \quad (2)$$

Here μ is the mass matrix of the up and down quarks, which has diagonal form: $\mu = \text{diag}(m_u, m_d)$. In the exact isospin symmetry case these masses are equal ($m_u = m_d = m$) and the μ matrix is proportional to the unit matrix. A matrix element of the nucleon isovector axial-vector current at finite temperature can be written analogous to the zero temperature case [3]:

$$\langle N(p', T) | j^{\mu,a}(0) | N(p, T) \rangle = \bar{u}(p') \left[\gamma^\mu \gamma^5 G_A(q^2, T) + \frac{q^\mu}{2m_N} \gamma^5 G_P(q^2, T) \right] \frac{\tau^a}{2} u(p). \quad (3)$$

Here $q_\mu = p'_\mu - p_\mu$ is the total momentum in the interaction vertex and m_N is the nucleon mass, $G_A(q^2, T)$ and $G_P(q^2, T)$ are called the axial-vector and induced pseudoscalar form factors respectively. Due to the Hermiticity of the $j^{\mu,a}$ current the form factors $G_A(q^2, T)$ and $G_P(q^2, T)$ are real functions of q^2 in the $q^2 \leq 0$ domain. We shall consider the $Q^2 = -q^2$ timelike momentum domain. Here we consider the form factor $G_A(q^2, T)$ at finite temperature in the soft-wall AdS/QCD model framework.

III. SOFT-WALL MODEL AT FINITE TEMPERATURE

The action for the soft-wall model, which we use for our finite-temperature study, contains a dilaton field φ depending on the temperature:

$$S = \int d^4x dz \sqrt{g} e^{-\varphi(z,T)} L(x, z, T), \quad (4)$$

where g denotes $g = |\det g_{MN}|$, (for $M, N = 0, 1, 2, 3, 5$) and the extra dimension z varies in the range $0 \leq z < \infty$. The background geometry is assumed to be 5D AdS space-time with the metric at finite temperature:

$$ds^2 = e^{2A(z)} \left[f(z, T) dt^2 - d\vec{x}^2 - \frac{dz^2}{f(z, T)} \right]. \quad (5)$$

Here $x = (t, \vec{x})$ is the set of Minkowski coordinates, z is the holographic coordinate, $A(z) = \log(\frac{R}{z})$, and R is the AdS radius. The thermal factor $f(z, T)$ has a form [37]:

$$f(z, T) = 1 - \frac{z^4}{z_H^4}, \quad (6)$$

where z_H is the position of the event horizon and it is related to the Hawking temperature as $T = 1/(\pi z_H)$. The dilaton field $\varphi(z) = k^2 z^2$, where k is a scale parameter of a few hundred MeV, was introduced to make the integral over the z finite at IR boundary ($z \rightarrow \infty$). For the finite-temperature soft-wall model, the form of the dilaton has been modified by including the temperature-depending terms. In this model it is convenient to apply the Regge-Wheeler tortoise coordinate r ,

$$r = \int \frac{dz}{f(z)} \quad (7)$$

instead of z [49], and to neglect the terms of higher order than T^8 in the expansion of z . This gives following relation between the r and z coordinates [26]:

$$r \approx z \left[1 + \frac{z^4}{5z_H^4} + \frac{z^8}{9z_H^8} \right]. \quad (8)$$

The metric for the AdS-Schwarzschild space-time in these coordinates will be written in the form:

$$ds^2 = e^{2A(r)} f^{\frac{3}{5}}(r) \left[dt^2 - \frac{(d\vec{x})^2}{f(r)} - dr^2 \right] \quad (9)$$

with $A(r) = \log(\frac{R}{r})$. The thermal factor $f(r)$ depending on the r coordinate has same form as in Eq. (7):

$$f(r) = 1 - \frac{r^4}{r_H^4}. \quad (10)$$

The thermal version of the usual quadratic dilaton was applied in Ref. [36]

$$\varphi(r, T) = K^2(T) r^2 \quad (11)$$

and this idea was developed further in Refs. [26–29]. As expected, setting $T = 0$ the terminal dilaton is reduced to the usual one $\varphi(r, 0) = k^2 r^2$. The $K^2(T)$ parameter in Eq. (11) is the

parameter of spontaneous breaking of chiral symmetry and its explicit form was established in Refs. [26–29]

$$K^2(T) = k^2[1 + \rho(T) + O(T^6)]. \quad (12)$$

In section VI, we shall substantiate the $K^2(T)$ dependence in Eq. (12) and will give some more details of this relation. The $\rho(T)$ function encodes the T dependence of the dilaton field and was found in the form

$$\rho(T) = \frac{9\alpha\pi^2}{16} \frac{T^2}{12F^2} - \frac{N_f^2 - 1}{N_f} \frac{T^2}{12F^2} - \frac{N_f^2 - 1}{2N_f^2} \left(\frac{T^2}{12F^2} \right)^2 + O(T^6). \quad (13)$$

Here $N_f = 2$ is the number of quark flavors. The pion decay constant F is proportional to the k parameter $F = \frac{k\sqrt{6}}{8}$ [39]. The parameter α parametrizes the thermal correction proportional to the z^2 dependence. It encodes the contribution of gravity to the restoration of chiral symmetry at the critical temperature $T_c = 0.2$ GeV and gets small values.

IV. MESON PROPAGATOR AT FINITE TEMPERATURE

It is known from the zero-temperature case, the EOM for the A_M axial-vector field in the soft-wall model coincides with the one for the V_M vector field at certain limits ($m_q \rightarrow 0, z \rightarrow z_{UV}$) [17],[30]. Of course, the bulk-to-boundary propagators, which are the solutions of the equations for the A_M and V_M fields, also will coincide at this approximation. At finite temperature case, in the soft-wall model with the thermal dilaton, we have formal replacements $z \rightarrow r, k \rightarrow K(T)$, which do not change the EOMs. Consequently, the known expression for the vector bulk-to-boundary propagator at finite temperature obtained in Ref. [26] can be used for the axial-vector field's propagator as well. In the soft-wall model with the thermal dilaton field $\varphi(r, T)$ defined in Eq. (11), the EOM for a vector field was obtained in the following form [26, 27]:

$$\partial_r \left(\frac{e^{-\varphi(r, T)}}{r} \partial_r A(Q, r, T) \right) - Q^2 \frac{e^{-\varphi(r, T)}}{r} \partial_r A(Q, r, T) = 0. \quad (14)$$

The $A(Q, r, T)$ thermal propagator $A(Q, r, T)$ satisfies the boundary condition $A(Q, z = 0, T) = 1$. Here Q is the momentum transfer. Eq. (14) is similar to one at zero temperature, and the only difference between them is the T -dependence of the dilaton parameter. So, the solution of the Eq. (14) written as [27]

$$A(Q, r, T) = \Gamma(1 + a(Q, T)) U(a(Q, T), 0, K^2 r^2) = K^2 r^2 \int_0^1 \frac{dx}{(1-x)^2} x^{a(Q, T)} e^{-K^2 r^2 \frac{x}{1-x}}, \quad (15)$$

is the bulk-to-boundary propagator for the axial-vector field too. Here Γ is Euler's gamma function and $a(Q, T) = \frac{Q^2}{4K^2(T)}$. $U(x, y, z)$ is a Tricomi function, also known as the confluent hypergeometric function of the second kind.

V. NUCLEONS AT FINITE TEMPERATURE

In this section, we briefly present the profile function for a fermion field in the model with thermal dilaton, which was derived in the Ref. [27]. Action for the bulk fermion field in this model is written in the form:

$$S = \int d^4x dr e^{-\varphi(r, T)} \sqrt{g} \bar{\Psi}(x, r, T) D_{\pm}(r) \Psi(x, r, T). \quad (16)$$

Here $D_{\pm}(r) = \frac{i}{2} \Gamma^M [\partial_M - \frac{1}{4} \omega_M^{ab} [\Gamma_a \Gamma_b]] \mp [\mu(r, T) + U_F(r, T)]$ are covariant derivatives, which include five-dimensional temperature-dependent mass $\mu(r, T) = \mu f^{\frac{3}{10}}(r, T)$. $\mu = N_B + L - \frac{3}{2}$, where $N_B = 3$ and L are the number of partons and orbital angular momentum ($L = 0$) of the nucleons, respectively. Thermal potential for nucleons $U_F(r, T)$ is defined as $U_F(r, T) = \varphi(r, T)/f^{\frac{3}{10}}(r, T)$. Non-zero components of the spin connection ω_M^{ab} are given by $\omega_M^{ab} = (\delta_{\mu}^a \delta_r^b - \delta_{\mu}^b \delta_r^a) r f^{\frac{1}{5}}(r, T)$. Commutator of the Dirac matrices is defined by $\sigma^{MN} = [\Gamma^M, \Gamma^N]$ and $\Gamma^M = e_a^M \Gamma^a$, where $e_a^M = z \delta_a^M$ is the inverse vielbein. The Γ^a matrices are defined as $\Gamma^a = (\Gamma^{\mu}, -i\Gamma^5)$. The Ψ field is decomposed into the left and right chirality components as $\Psi(x, r, T) = \Psi^R(x, r, T) + \Psi^L(x, r, T)$, with definition $\Psi^{L,R}(x, r, T) = \frac{1 \mp \gamma^5}{2} \Psi$, where $\gamma^5 \Psi^L = -\Psi^L$, $\gamma^5 \Psi^R = \Psi^R$. Kaluza-Klein decomposition of the $\Psi^{L,R}$ fields is written as $\Psi^{L,R} = \sum_n \Phi_n^{L/R}(r, T) \psi_n(x)$, where $\Phi_n^{L/R}(r, T)$ are the profile functions and 4D wave functions $\psi_n(x)$ satisfy free Dirac equation $\not{p} \psi_n(x) = M_n(0) \psi_n(x)$. In the further calculations, the following replacement in the profile functions is useful [27]:

$$\Phi_n^{L/R}(r, T) = e^{-\frac{3}{2}A(r)} F_n^{L/R}(T). \quad (17)$$

EOM obtained from the action in Eq. (16) is the 5D Dirac equation at finite temperature. Substituting $\Phi_n^{L/R}(r, T)$ in the EOM the following equation is obtained for the $F_n^{L/R}(r, T)$ profiles in the nucleon's rest frame [27]:

$$\left[\partial_r^2 + U_{L/R}(r, T) \right] F_n^{L/R}(r, T) = M_n^2(T) F_n^{L/R}(r, T). \quad (18)$$

Here $U_{L,R}(r, T)$ are the effective potentials are written in the sum of the zero- and finite-temperature terms:

$$U_{L/R}(r, T) = U_{L/R}(r) + \Delta U_{L/R}(r, T) \quad (19)$$

with the explicit forms

$$U(r) = k^4 r^2 + \frac{(4m^2 - 1)}{4r^2}, \quad \Delta U(r, T) = 2\rho(T)k^4 r^2. \quad (20)$$

Here $m = N + L - 2$ and for the nucleon with three parton it equals to $m = L + 1$. M_n^2 in the Eq. (18) is the nucleon mass spectrum, and at the low temperatures can also be written as the sum of the zero- and finite-temperature parts:

$$M_n^2(T) = M_n^2(0) + \Delta M_n^2(T), \quad (21)$$

in which the terms have the explicit forms respectively

$$M_n^2(0) = 4k^2 \left(n + \frac{m+1}{2} \right), \quad (22)$$

$$\Delta M_n^2(T) = \rho(T)M_n^2(0) + \frac{R\pi^4 T^4}{k^2}, \quad R = (6n - 1)(m + 1). \quad (23)$$

Equation (18) is solved using the boundary conditions on $F_n^{L/R}(r, T)$ in the ultraviolet (UV) and infrared (IR) limits at small r

$$F_n^{L/R}(r, T) \sim r^{N+L-1 \pm \frac{1}{2}}, \quad (24)$$

and at large r

$$F_n^{L/R}(r, T) \rightarrow 0. \quad (25)$$

The normalization conditions for the profile functions $F_n^{L/R}(r, T)$ are:

$$\int_0^\infty dr e^{-3A(r)} \Phi_m^{L,R}(r, T) \Phi_n^{L,R}(r, T) = \int_0^\infty dr F_m^{L,R}(r, T) F_n^{L,R}(r, T) = \delta_{mn}. \quad (26)$$

In general case the Schrodinger-type equations (18) have following analytical solutions:

$$F_n^{L/R}(r, T) = \sqrt{\frac{2\Gamma(n+1)}{\Gamma(n+m_{L/R}+1)}} K^{m_{L/R}+1} r^{m_{L/R}(T)+\frac{1}{2}} e^{-\frac{K^2 r^2}{2}} L_n^{m_{L/R}}(K^2 r^2). \quad (27)$$

By taking $m_{L/R} = m \pm \frac{1}{2}$ in it, we obtain an expression for the profile functions of the nucleons, which coincide with $T \rightarrow 0$ limit with the ones obtained in Ref. [40] for the $T = 0$ case.

VI. CONDENSATE, DILATON AND CHIRAL SYMMETRY BREAKING

The action for the pseudo-scalar X field in AdS/QCD has a form:

$$S = \int_0^\infty d^5 x \sqrt{g} e^{-\varphi(z)} \text{Tr} \{ |DX|^2 - m_5^2 |X|^2 \}. \quad (28)$$

In terms of the tortoise coordinate r and with the thermal dilaton this action will slightly change:

$$S_X = \int d^4x dr \sqrt{g} e^{-\varphi(r,T)} \text{Tr} \left[|DX|^2 + 3|X|^2 \right], \quad (29)$$

where DX is the covariant derivative including the interaction with the gauge fields $A_{L,R}$. In terms of the vector M_M and the axial-vector A_M fields the covariant derivative looks like: $D^M X = \partial^M X - iA_L^M X + iXA_R^M = \partial^M X - i[M_M, X] - i\{A_M, X\}$, $A_{L,R}^M = A_{L,R}^M t^a$ and $F_{L,R}^{MN}$ are the field strengths of these fields. The X field transforms under the bifundamental representation of the flavor symmetry group $SU(2)_L \times SU(2)_R$ of the model and performs the breaking of the chiral symmetry by Higgs mechanism [42]. EOM for the X field, which is obtained from Eq. (28), has a solution

$$\langle X \rangle = \frac{1}{2} v(z), \quad (30)$$

where

$$v(z) = \frac{1}{2} M_q a z + \frac{1}{2a} \Sigma z^3. \quad (31)$$

Here $a = \sqrt{N_c}/(2\pi)$ ($N_c = 3$) is the normalization parameter [47]. According to dictionary of the bulk/boundary correspondence, the parameters M_q and Σ are identified with the u, d quark mass matrix and with the chiral condensate $\Sigma = \langle 0 | \bar{q}q | 0 \rangle$, correspondingly. For the finite-temperature case the quark condensate within $v(z)$ in Eq. (31) has depending on temperature and the z coordinate should be replaced by r . Then, the $v(r, T)$ solution has a form:

$$v(r, T) = \frac{1}{2} M_q a r + \frac{1}{2a} \Sigma(T) r^3. \quad (32)$$

T -dependence of the quark condensate, which was found in Ref. [39] using two-loop chiral perturbation theory at finite temperature, has been applied in the Refs. [26, 27] for the finite-temperature soft-wall model. It has a form:

$$\Sigma(T) = \Sigma \left[1 - \frac{N_f^2 - 1}{N_f} \frac{T^2}{12F^2} - \frac{N_f^2 - 1}{2N_f^2} \left(\frac{T^2}{12F^2} \right)^2 + O(T^6) \right] = \Sigma [1 + \Delta_T + O(T^6)], \quad (33)$$

where N_f is the number of quark flavors and F is the pion decay constant. It can be seen that $\Delta(T) = -\frac{N_f^2 - 1}{N_f} \frac{T^2}{12F^2} - \frac{N_f^2 - 1}{2N_f^2} \left(\frac{T^2}{12F^2} \right)^2$ in Eq. (33) is related with the $\rho(T)$ in Eq. (13). In the soft-wall model the dilaton field $\varphi(r)$ is responsible for the dynamical breaking of the chiral symmetry. The chiral quark condensate $\Sigma(T)$ is the result of chiral symmetry breaking. Both constants K and Σ depend only on T . Therefore, it was supposed in Refs. [26, 27] that the T -dependence of the dilaton parameter $K^2(T)$ should be the same as the one of the $\Sigma(T)$ quark condensate:

$$K^2(T) = k^2 \frac{\Sigma(T)}{\Sigma}. \quad (34)$$

It was also conjectured that known relation at $T = 0$

$$\Sigma = -N_f B F^2 \quad (35)$$

holds at the $T \neq 0$ case too:

$$\Sigma(T) = -N_f B(T) F^2(T). \quad (36)$$

Here B is the condensate parameter. Then, as a result of Eqs. (11) and (34) the T -dependence of the $\Sigma(T)$ condensate can be expressed in terms of the $\Delta(T)$ function [42]:

$$\Sigma(T) = \Sigma [1 + \Delta(T)]. \quad (37)$$

Let us note, that the relation (37) is valid up to T^6 degree of the temperature. The $F(T)$ and $B(T)$ dependencies have been studied in the Ref. [27].

VII. HOLOGRAPHY AND THE BULK INTERACTION LAGRANGIAN

We can apply the holography principle to get the G_A form factor in the boundary QCD from the bulk interaction action:

$$S_{int} = \int d^5x \sqrt{g} L_{int}. \quad (38)$$

The generating functional Z_{AdS} of the bulk theory is defined by the classical bulk action S_{int} :

$$Z_{AdS} = e^{iS_{int}}. \quad (39)$$

AdS/CFT correspondence identifies the generating functional Z_{AdS} with the generating function Z_{QCD} of the boundary QCD [50]:

$$Z_{AdS} = Z_{QCD}. \quad (40)$$

Using the holographic identification in Eq. (40), one can find the $\langle J_\mu^a \rangle^{QCD}$ axial-vector current of nucleons in the boundary QCD theory after calculating S_{int} for the bulk theory. The variation derivative of the gravity functional Z_{AdS} over the A_μ^0 field will give us sought current:

$$\langle J_\mu^a \rangle^{QCD} = -i \frac{\delta Z_{AdS}}{\delta A_\mu^{a(0)}} \Big|_{A_\mu^{a(0)}=0}. \quad (41)$$

Here $A_\mu^{(0)}$ is the UV boundary value of the A_μ bulk axial-vector field and has an interpretation of a wave function of the axial-vector meson at the boundary. The axial-vector current

$J_\mu^a(p', p) = G_A \bar{u}(p') \gamma^5 \gamma_\mu (\tau^a/2) u(p)$ obtained from the (41) contains the G_A factor, which is the integral over the r coordinate and depends on Q^2 . According to AdS/CFT correspondence the $\bar{u}(p') \gamma^5 \gamma_\mu (\tau^a/2) u(p)$ current is the axial-vector current of the nucleons. Consequently, the $G_A(Q^2)$ factor is accepted as the axial-vector form factor of the nucleons. This correspondence is relevant for the bulk theory at finite temperature as well.

Now, the main question is how to determine an explicit form of the L_{int} interaction Lagrangian between the A_M , X , and $\Psi_{1,2}$ fields in the bulk theory. It is possible to construct different Lagrangian terms, which describe the different interactions between these fields. However, we are interested in that interaction terms, which produce namely the axial-vector current Eq. (1) in the boundary theory. These terms should be proportional to the A_M axial-vector field because of the P invariancy of the Lagrangian and be 5D Lorentz invariant. The necessary terms can be taken from the zero-temperature case and then extended to the finite-temperature case by replacing the fields at $T = 0$ with the thermal ones. The interactions between the bulk fields A_M , X , and $\Psi_{1,2}$ at zero-temperature case presented in the Refs. [21],[20],[8],[22, 25, 48], will contribute to the finite-temperature $G_A(Q^2, T)$ form factor as well. These terms are following ones: 1) a minimal coupling term

$$L^{(1)} = \bar{\Psi}_1 \Gamma^M (A_L)_M \Psi_1 - \bar{\Psi}_2 \Gamma^M (A_R)_M \Psi_2 = \frac{1}{2} \left(\bar{\Psi}_1 \Gamma^M A_M \Psi_1 - \bar{\Psi}_2 \Gamma^M A_M \Psi_2 \right), \quad (42)$$

2) a magnetic gauge coupling term

$$\begin{aligned} L^{(2)} &= ik_1 \left\{ \bar{\Psi}_1 \Gamma^{MN} (F_L)_{MN} \Psi_1 - \bar{\Psi}_2 \Gamma^{MN} (F_R)_{MN} \Psi_2 \right\} \\ &= \frac{i}{2} k_1 \left\{ \bar{\Psi}_1 \Gamma^{MN} F_{MN} \Psi_1 + \bar{\Psi}_2 \Gamma^{MN} F_{MN} \Psi_2 \right\}, \end{aligned} \quad (43)$$

where $F_{MN} = \partial_M A_N - \partial_N A_M$ is the field stress tensor of the axial-vector field A_M .

3) Three-field interaction term, which was introduced in Ref. [20]:

$$\begin{aligned} L^{(3)} &= \frac{g_Y}{2} \left[\bar{\Psi}_1 X \Gamma^M (A_L)_M \Psi_2 - \bar{\Psi}_2 X^\dagger \Gamma^M (A_R)_M \Psi_1 + h.c. \right] \\ &= g_Y \left(\bar{\Psi}_1 X \Gamma^M A_M \Psi_2 + \bar{\Psi}_2 X^\dagger \Gamma^M A_M \Psi_1 \right). \end{aligned} \quad (44)$$

Last term describes an interaction of three bulk fields at one point, and at the boundary, it corresponds to the nucleon-double meson interaction. Since this interaction is the chirality-changing one, the Yukawa coupling constant g_Y was chosen as the coupling constant in this term. Direct calculations show $L^{(3)}$ contributes to the axial-vector form factor of nucleons.

VIII. G_A FORM FACTOR AT FINITE TEMPERATURE

We write the action terms in the momentum space, using the

$$j^{5\mu}(p', p) = \bar{u}(p') \gamma^5 \gamma^\mu \frac{\tau^a}{2} u(p) \quad (45)$$

short notation for the axial-vector current. Let's list the $S^{(i)}$ action terms corresponding to the $L^{(i)}$ Lagrangians:

$$\begin{aligned} 1) S^{(1)} &= \frac{1}{2} \int d^4x \int_0^\infty dr \sqrt{g} \left\{ \bar{\Psi}_1 \Gamma^\mu A_\mu \Psi_1 - \bar{\Psi}_2 \Gamma^\mu A_\mu \Psi_2 \right\} \\ &= \frac{1}{2} \int d^4p d^4p' j^{5\mu}(p', p) A_\mu^a(Q) \int_0^\infty dr A(Q, r, T) \left[|F_{1R}(r, T)|^2 - |F_{1L}(r, T)|^2 \right], \end{aligned} \quad (46)$$

$$\begin{aligned} 2) S^{(2)} &= \frac{i}{4} k_1 \int d^4x \int_0^\infty dr \sqrt{g} \left\{ \bar{\Psi}_1 [\Gamma^5, \Gamma^\mu] \partial_5 A_\mu \Psi_1 + \bar{\Psi}_2 [\Gamma^5, \Gamma^\mu] \partial_5 A_\mu \Psi_2 \right\} \\ &= \frac{k_1}{2} \int d^4p d^4p' j^{5\mu}(p', p) A_\mu^a(Q) \int_0^\infty dr r (\partial_r A(Q, r, T)) \left[|F_{1R}(r, T)|^2 + |F_{1L}(r, T)|^2 \right], \end{aligned} \quad (47)$$

$$\begin{aligned} 3) S^{(3)} &= g_Y \int d^4x \int_0^\infty dr \sqrt{g} \left\{ \bar{\Psi}_1 X \Gamma^\mu A_\mu \Psi_2 + \bar{\Psi}_2 X^\dagger \Gamma^\mu A_\mu \Psi_1 \right\} \\ &= g_Y \int d^4p d^4p' j^{5\mu}(p', p) A_\mu^a(Q) \int_0^\infty dr A(Q, r, T) 2v(r, T) F_{1L}(r, T) F_{1R}(r, T). \end{aligned} \quad (48)$$

Here the both ($\bar{\Psi}$ and Ψ) bulk fermions are considered on the mass shell ($|p| = |p'| = m$), and m are the masses of the initial and final nucleons. Total action $S_{int} = S^{(1)} + S^{(2)} + S^{(3)}$ will produce the axial-vector form factor G_A of the nucleons at finite temperature. Taking derivatives over $A_\mu^a(Q)$ from the $S^{(i)}$ action terms we get the $G_A^{(i)}(T)$ contributions of these terms into the the axial-vector form factor $G_A(Q^2, T)$:

$$1) G_A^{(1)}(Q^2, T) = \frac{1}{2} \int_0^\infty dr A(Q, r, T) \left[|F_{1R}(r, T)|^2 - |F_{1L}(r, T)|^2 \right], \quad (49)$$

$$2) G_A^{(2)}(Q^2, T) = \frac{k_1}{2} \int_0^\infty dr r (\partial_r A(Q, r, T)) \left[|F_{1R}(r, T)|^2 + |F_{1L}(r, T)|^2 \right], \quad (50)$$

$$3) G_A^{(3)}(Q^2, T) = \frac{1}{2} g_Y \int_0^\infty dr A(Q, r, T) v(r) F_{1L}(r, T) F_{1R}(r, T). \quad (51)$$

$$G_A(Q^2, T) = G_A^{(1)}(Q^2, T) + G_A^{(2)}(Q^2, T) + G_A^{(3)}(Q^2, T). \quad (52)$$

IX. AXIAL-VECTOR TRANSITION FORM FACTOR

A formalism for the study of the nucleon resonances within holographic model has been proposed in Refs. [56–60]. For the transition form factor we apply the interaction Lagrangians (42)-(44).

However, this time the $\bar{\Psi}_{1,2}$ states describe the excited nucleon states, while $\Psi_{1,2}$ ones are the ground states. So, in the profile functions $F_{1,2L}^{(n)*}$ we take $n = 1$ and for this KK mode the mass of the excited nucleon is ($|p'| = m^*$). In the profile functions $F_{1,2L}^{(n)}$ we set $n = 0$ and ($|p| = m$). Contributions of the $G_{AT}^{(i)}(T)$ terms to the axial-vector transition form factor $G_{AT}(Q^2, T)$ have the forms:

$$1) G_{AT}^{(1)}(Q^2, T) = \frac{1}{2} \int_0^\infty dr A(Q, r, T) \left[\left(F_{1L}^{(n)*} F_{1L}^{(m)} - F_{2L}^{(n)*} F_{2L}^{(m)} \right) \right] \quad (53)$$

$$2) G_{AT}^{(2)}(Q^2, T) = \frac{k_1}{2} \int_0^\infty dr \partial_r A(Q, r, T) \left[\left(F_{1L}^{(n)*} F_{1L}^{(m)} + F_{2L}^{(n)*} F_{2L}^{(m)} \right) \right] \quad (54)$$

$$3) G_{AT}^{(3)}(Q^2, T) = \frac{1}{4} g_Y \int_0^\infty dr A(Q, r, T) v(r, T) \left[\left(F_{1L}^{(n)*} F_{1R}^{(m)} - F_{2L}^{(n)*} F_{2R}^{(m)} \right) \right]. \quad (55)$$

$$G_{AT}(Q^2, T) = G_{AT}^{(1)}(Q^2, T) + G_{AT}^{(2)}(Q^2, T) + G_{AT}^{(3)}(Q^2, T). \quad (56)$$

There are following relations between the profile functions of the first and second bulk fermion fields: $F_{1L} = F_{2R}$, $F_{1R} = -F_{2L}$.

X. NUMERICAL RESULTS

In Figs. 1-5 we present the dependencies of the normalized $G_A(Q^2, T)/G_A(0, 0)$ form factor on T and Q^2 for the ground state ($n = 0$) and the first excited state ($n = 1$) of nucleons in the left and right panels correspondingly. We depicted in Fig.4 the T -dependence of the $G_A(T)/G_A(0)$ form factor at $Q^2 = 0$ and at few fixed values of α . The aim of this analysis is to understand an impact of the parameter α on the shape of the T -dependency of the form factor at $Q^2 = 0$. In Fig.5 we present the Q^2 -dependency of the $G_A(Q^2)/G_A(0)$ form factor at fixed values $T = 0, 0.1, 0.17$ GeV. This analysis shows more clearly how the shape of the Q^2 -dependency deforms on small change of T . In order to expand our idea we also present the T and Q^2 dependencies of the normalized transition $G_{AT}(Q^2, T)/G_{AT}(0, 0)$ form factor at different value of α in Figs. 7 and Q^2 -dependency of $G_{AT}(Q^2)/G_{AT}(0)$ at different value of T , T -dependency of $G_{AT}(T)/G_{AT}(0)$ ($Q^2 = 0$) at different value of α at the right side in Fig. 8.

In numerical calculations the values of light quark mass m_q and quark condensate Σ are taken the values $m_q = 0.00234$ GeV and $(\Sigma)^{1/3} = 0.311$ GeV respectively, [43]. The constant $k_1 = -0.98$ was taken from [41], which was obtained from the fitting of the couplings $g_{\pi NN}$ and $g_{\rho NN}$ of

AdS/QCD model with the experimental data. For the Yukawa constant the value $g_Y = 9.182$ is used, which was taken from the Ref. [46].

From the presented figures 1-3 it follows the form factor graphs at different values of α have the same shape for the ground and excited states correspondingly. It means that the impact of the quantum number n and the parameter α to the shape of the form factor is weak enough. Another observation is that in the all T -dependency graphs the G_A form factor goes to zero around the $T_c = 0.2$ GeV. This is interpreted with the hadron melting at the temperature of confinement-deconfinement phase transition.

Main aim of present work is to study an influence of the medium temperature on the G_A form factor. Since there is no experimental data³ for the G_A form factor at finite temperature, in Fig. 6 we present a comparison of our result for $G_A(Q^2)/G_A(0)$ at $T = 0$ with the hard-wall AdS QCD model result for the $G_A(Q^2)$ form factor [20, 51], experimental data [3, 52] and result of the Light Cone Sum Rules (LCSR) [6]. All theoretical predictions for the Q^2 dependencies have the form $1/Q^n$ dependence, which is typical for the nucleon form factors. Experimental data for G_A exist in two different intervals of Q^2 , in $0.075 \text{ GeV}^2 \leq Q^2 \leq 1 \text{ GeV}^2$ ([3]) and in $2 \text{ GeV}^2 \leq Q^2 \leq 4 \text{ GeV}^2$ ([52]). There is no momentum restriction on the applicability of holographic models, while other theoretical approaches, as light cone sum rules, are applicable only for $Q^2 \geq 1 \text{ GeV}^2$. The theoretical dependencies obtained from the hard- and soft-wall models cover both momentum intervals of the experiment. It is seen from Fig.6, that holographic model predictions for the Q^2 dependence of the G_A form factor are in a good agreement with the experimental data and other theoretical approaches. In Fig. 7 the axial vector transition form factor $G_{AT}(Q^2, T)/G_{AT}(0, 0)$ was plotted at the parameter values $\alpha = 0.1, 0.2, 0.3$. This analysis shows a weak dependence on the parameter α of the form factor. The graphs have similar shapes as in Fig. 1 -3. In Fig. 8 in the left side the Q^2 dependence of the transition form factor $G_{AT}(Q^2)/G_{AT}(0)$ was plotted at some fixed values of T . In the right side the T dependence of the zero-momentum transition form factor $G_{AT}(T)/G_{AT}(0)$ was plotted at different values of the parameter α , respectively. The analysis shows that as α decreases, the curvature of the graph increases.

³ The only theoretical result for the temperature-dependent $g_a(t)$ coupling constant is Ref. [31], which based on QCD Sum Rules. In their another work (Ref. [54]) the authors express that this result contrasts to other effective hadronic couplings ([53, 55]) and diverges when $T \rightarrow T_c$. This result also disagree with the soft-wall model result on coupling (form factor) vanishing at T_c observed in [26–30].

XI. SUMMARY

In the present work, we investigate the temperature dependency of the axial-vector form factor in the framework of the soft-wall AdS/QCD model containing the thermal dilaton field. Numerical analysis shows that the form factor value decreases by the increment of temperature. This result may have a use for the nucleon-axial-vector meson interaction studies at a finite temperature.

-
- [1] U. Mosel, *Ann. Rev. Nucl. Part. Sci.* **66**, (2016).
 - [2] L. Alvarez-Ruso, et al., *Prog. Part. Nucl. Phys.* **100**, (2018).
 - [3] V. Bernard, L. Elouadrhiri and U.-G. Meissner, *J.Phys. G***28**, R1 (2002).
 - [4] C. Alexandrou, M. Brinet, J. Carbonell, M. Constantinou, P. A. Harraud, P. Guichon, K. Jansen, T. Korzec and M. Papinutto, *Phys. Rev. D***83** 045010 (2011).
 - [5] G. Eichmann, H. Sanchis-Alepuz, R. Williams, R. Alkofer and C. S. Fischer, *Prog.Part.Nucl. Phys.* **91**, (2016).
 - [6] I.V. Anikin, V.M. Braun and N. Offen, *Phys. Rev. D* **94**, 034011 (2016).
 - [7] A. S. Meyer, M. Betancourt, R. Gran and R.J. Hill, *Phys.Rev. D* **93**, (2016).
 - [8] G. Ramalho, *Phys.Rev. D* **94**, (2018).
 - [9] C. Chen, Christian S. Fischer, Craig D. Roberts, J. Segovia, *Phys. Lett. B*, **815**, 136150 (2021).
 - [10] J. M. Maldacena, *Int. J. Theor. Phys.* **38**, 1113 (1999).
 - [11] S.S. Gubser, I.R. Klebanov and A. M. Polyakov, *Phys. Lett. B* **428**, 105 (1998).
 - [12] E. Witten, *Adv. Theor. Math. Phys.* **2**, 253 (1998).
 - [13] H. Boschi-Filho and N.R.F. Braga, *J.High Energy Phys.* **0305**, 009 (2003).
 - [14] H. Boschi-Filho and N.R.F. Braga, *Eur. Phys. J. C* **32** (2004).
 - [15] J. Erlich, E. Katz, D. T. Son and M. A. Stephanov, *Phys. Rev. Lett.* **95**, 261602 (2005).
 - [16] L. Da Rold and A. Pomarol, *Nucl. Phys.B* **721**, 79 (2005).
 - [17] L. Da Rold and A. Pomarol, *J. High Energy Phys.* **0601**, 157 (2006).
 - [18] A. Karch, E. Katz, D.T. Son and M. A. Stephanov, *Phys. Rev. D* **74**, 015005 (2006).
 - [19] S.J. Brodsky, G. F. de Teramond, H.G. Dosch and J. Erlich, *Int. J. Theor. Phys.*, **56**, 2017.
 - [20] Sh. Mamedov, B.B. Sirvanli, I. Atayev, and N. Huseynova, *Int. J. Theor. Phys.* **54**, (2017).
 - [21] T. Gutsche, V. E. Lyubovitskij, I. Schmidt, A.Vega, *Phys.Rev. D* **86**, 036007 (2012).
 - [22] I. Atayev and Sh. Mamedov, *Izv. vuzov. Fizika*, v **64**, n **12**, 88 (2021).
 - [23] J. Leutgeb and A. Rebhan, *Phys. Rev. D* **101**, 114015 (2020).
 - [24] T. Gutsche, V. E. Lyubovitskij, I. Schmidt, and A. Y. Trifonov, *Phys. Rev. D* **99**, 054030 (2019).
 - [25] I. Atayev and Sh. Mamedov, work in progress
 - [26] T. Gutsche, V. E. Lyubovitskij, I. Schmidt, and A. Y. Trifonov, *Phys. Rev. D* **99**, 054030 (2019).

- [27] T. Gutsche, V. E. Lyubovitskij, I. Schmidt, and A. Y. Trifonov, *Phys. Rev. D* **99**, 114023 (2019).
- [28] T. Gutsche, V. E. Lyubovitskij, I. Schmidt, and A. Y. Trifonov, *Phys. Rev. D* **952**, 114934 (2020).
- [29] Sh. Mamedov and N. Nasibova, *Phys. Rev. D*, **104**, 036010 (2021).
- [30] Sh. Mamedov and Sh. Taghiyeva, *Eur. Phys. J. C* **81**, 1080 (2021).
- [31] C.A. Dominguez, M. Loewe, C. van Gend, *Phys.Lett. B***460**, 442, (1999).
- [32] P. Gysbers, G. Hagen, J.D. Holt, G.R. Jansen, T.D. Morris, *Nature Phys.* **15**, (2019)5, 428.
- [33] A. Lovato, J. Carlson, S. Gandolfi, N. Rocco, R. Schiavilla, *Phys. Rev. X* **10**, (2020) 031068.
- [34] G. B. King, L. Andreoli, S. Pastore, M. Piarulli, R. Schiavilla, R. B. Wiringa, J. Carlson, S. Gandolfi, *Phys. Rev. C* **102**, 025501 (2020).
- [35] Z. Abidin and C. Carlson, *Phys. Rev. D* **79**, 115003 (2009).
- [36] A. Vega and M. A. Martin Contreras, *Nucl. Phys. B* **942**, (2019).
- [37] E. Witten, *Adv. Theor. Math. Phys.* **2**, 253 (1998).
- [38] T. Branz, T. Gutsche, V. E. Lyubovitskij, I. Schmidt, and A. Vega, *Phys. Rev. D* **82**, 074022 (2010).
- [39] J. Gasser and H. Leutwyler, *Phys. Lett. B* **184**, 83 (1987).
- [40] T. Gutsche, V.E. Lyubovitskij, I. Schmidt, and A. Vega, *Phys. Rev. D* **85**, 076003 (2012).
- [41] H. C. Ahn, D. K. Hong, C. Park and S. Siwach, *Phys. Rev. D* **80**, 054001 (2009).
- [42] T. Gherghetta, J. I. Kapusta, and T. M. Kelley, *Phys. Rev. D* **79**, 076003 (2010).
- [43] N. Maru and M. Tachibana, *Eur. Phys. J. C* **63**, 123 (2009).
- [44] N. Huseynova and Sh. Mamedov, *Int. J. Theor. Phys.* **54**, 3799 (2015).
- [45] T. Gutsche, V.E. Lyubovitskij, I. Schmidt and A. Vega, *Phys. Rev. D* **86**, 036007 (2012).
- [46] D.K. Hong, H.-C. Kim, S. Siwach and H.-U. Yee, *J. High Energy Phys.*, **0711** 036 (2007).
- [47] A. Cherman, Th.D. Cohen and E.S. Werbos, *Phys. Rev. C* **79**, 045203, (2009).
- [48] N. Huseynova and Sh. Mamedov, *Int. J. Mod. Phys. A* **34** (2020) 35, 1950240.
- [49] T. Regge and J.A. Wheeler, *Phys. Rev.* **108**, 1063, (1957).
- [50] Makoto Natsuume, *AdS/CFT Duality User Guide*, *Lect.Notes Phys.* **903** (2015) pp.1-294.
- [51] N.J. Huseynova, *Meson and baryons interactions in the framework of ADS/QCD models*, Ph.D. dissertation, Baku State University, 2017.
- [52] K. Park et al. [CLAS Collaboration], *Phys. Rev. C* **85**, 035208 (2012).
- [53] C.A. Dominguez, C. van Gend, M. Loewe, *Phys.Lett. B***429**, 64 (1998)
- [54] C.A. Dominguez, C. van Gend, M. Loewe, *Nucl.Phys.B Proc.Suppl.* **86**, 413 (2000)
- [55] A. Ayala, C.A. Dominguez, M. Loewe, Y. Zhang, *Phys.Rev.D* **86**, 114036 (2012)
- [56] G. F. de Teramond and S. J. Brodsky, *AIP Conf. Proc.* **1432**, 168 (2012)
- [57] T. Gutsche, V. E. Lyubovitskij, I. Schmidt, and A. Vega, *Phys. Rev. D* **87**, 016017 (2013).
- [58] G. Ramalho and D. Melnikov, *Phys. Rev. D* **97**, 034037 (2018); G. Ramalho, *Phys. Rev. D* **96**, 054021 (2017).
- [59] G. Ramalho, *Phys. Rev. D* **96**, 054021 (2017).
- [60] T. Gutsche, V. E. Lyubovitskij and I. Schmidt, *Phys. Rev. D* **97**, 054011 (2018).

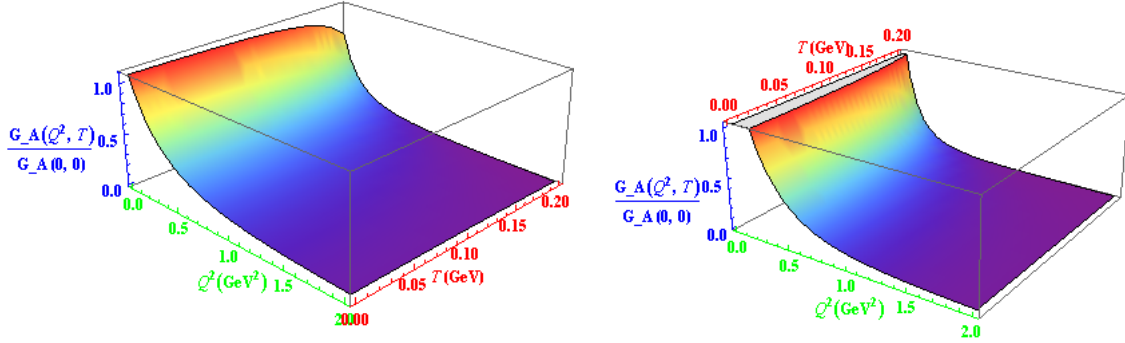


FIG. 1: $G_A(Q^2, T)/G_A(0, 0)$ form factor in the ground ($n = 0$) and excited states ($n = 1$) of the nucleons at $\alpha = 0.1$.

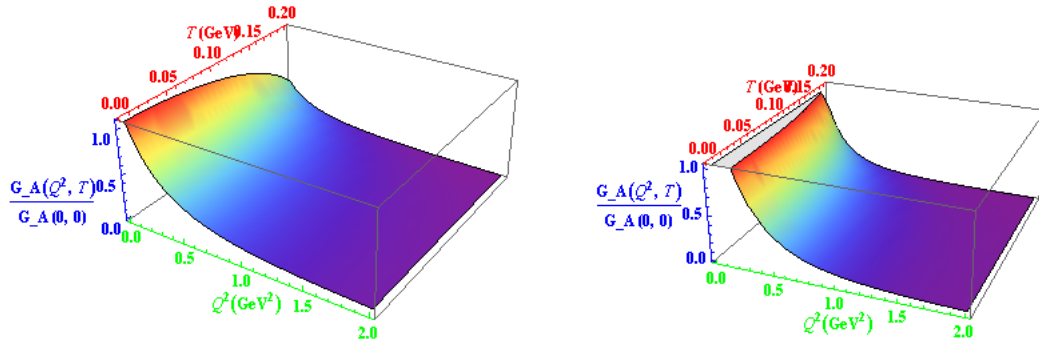


FIG. 2: $G_A(Q^2, T)/G_A(0, 0)$ form factor in the ground ($n = 0$) and excited states ($n = 1$) of the nucleons at $\alpha = 0.2$.

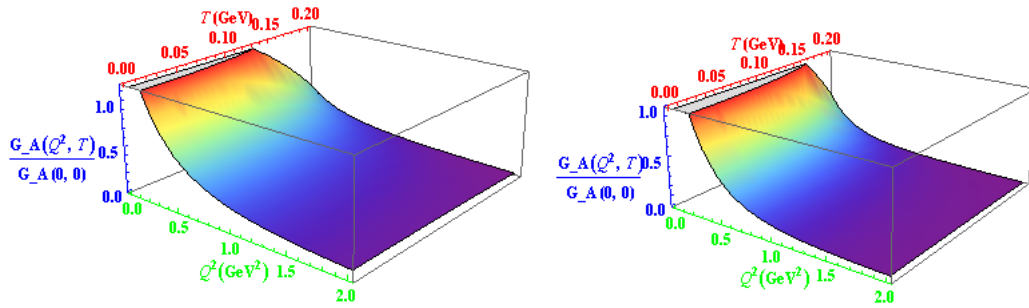


FIG. 3: $G_A(Q^2, T)/G_A(0, 0)$ form factor in the ground ($n = 0$) and excited states ($n = 1$) of the nucleons at $\alpha = 0.3$.

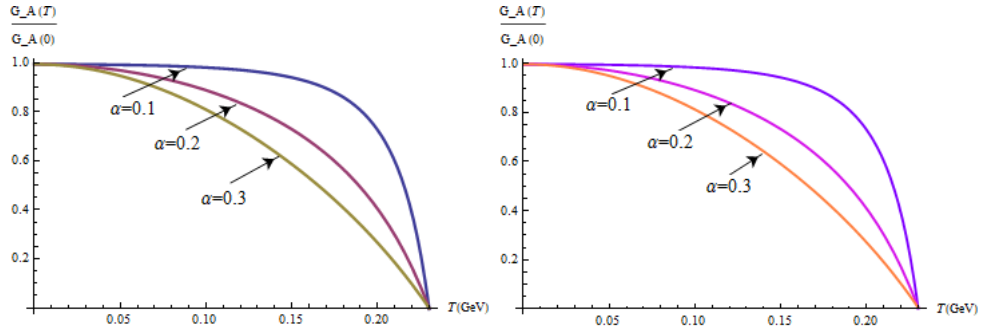


FIG. 4: $G_A(T)/G_A(0)$ form factors at $Q^2 = 0$ and different values of α in the ground ($n = 0$) and excited ($n = 1$) states of the nucleons.

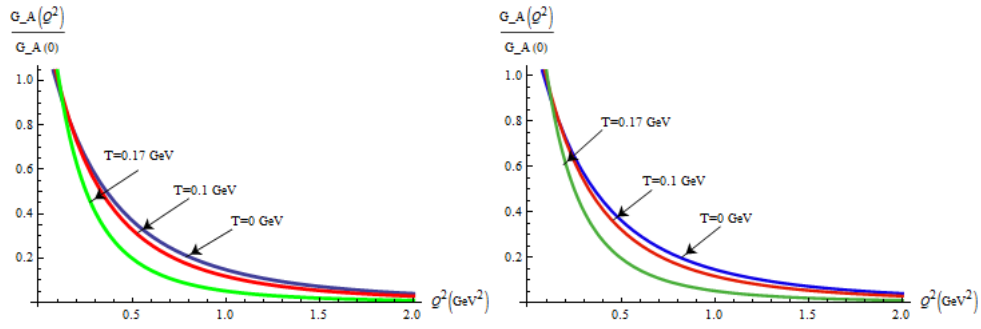


FIG. 5: $G_A(Q^2)/G_A(0)$ form factors at different values of T in the ground ($n = 0$) and excited ($n = 1$) states of the nucleons.

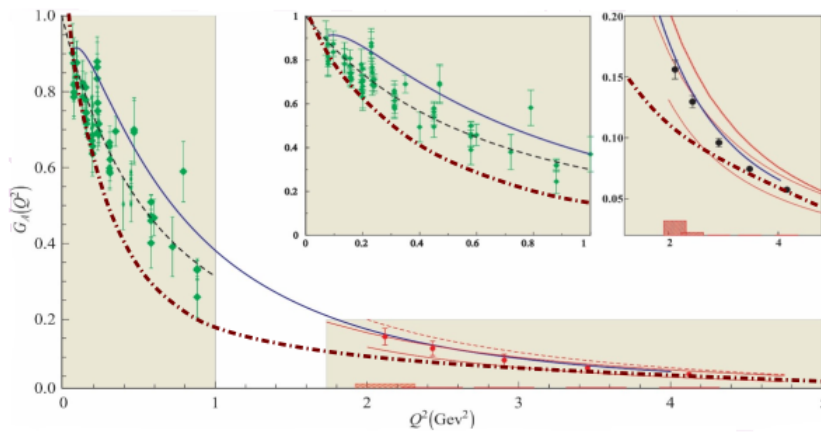


FIG. 6: Comparison of our result for the $G_A(Q^2, T = 0)/G_A(0, 0)$ form factor at $n = 0$ and $T = 0$ values (densely dashdotted line) with the hard-wall result obtained in [20, 51] (solid blue line), LCSR result in the $2 \leq Q^2 \leq 5$ interval (red dashed line and red solid line) ([6]) and experimental data taken from [3] and [52].

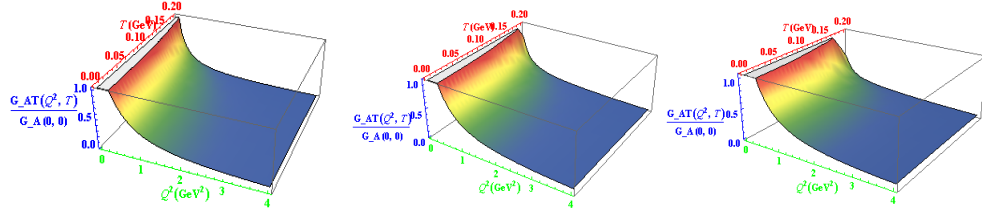


FIG. 7: $G_{AT}(Q^2, T)/G_{AT}(0, 0)$ transition form factor of nucleons at parameter values $\alpha = 0.1, 0.2, 0.3$, respectively.

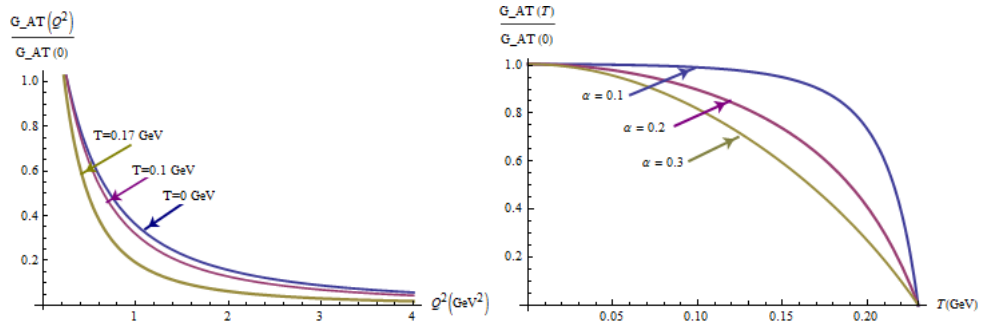


FIG. 8: Q^2 -dependence of transition form factor $G_{AT}(Q^2)/G_{AT}(0)$ at different values of T and the T -dependence of $G_{AT}(T)/G_{AT}(0)$ at different values of the parameter α , respectively.